A

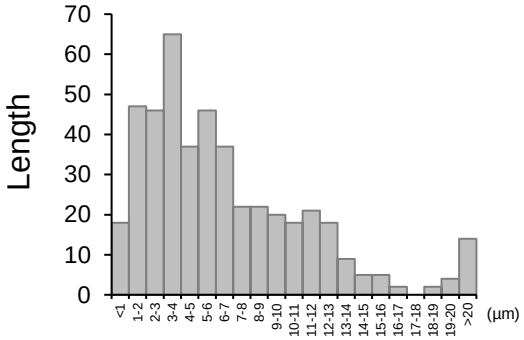

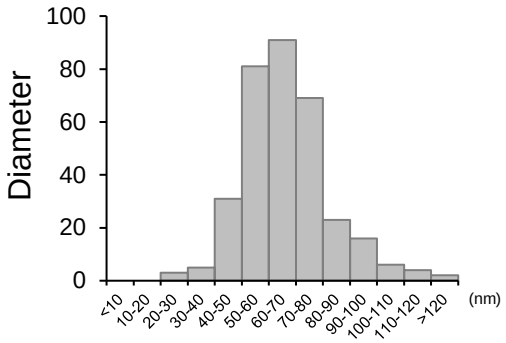

B

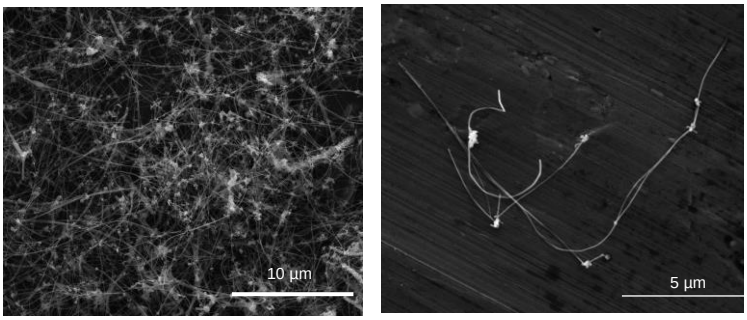

C Sequential necropsies test

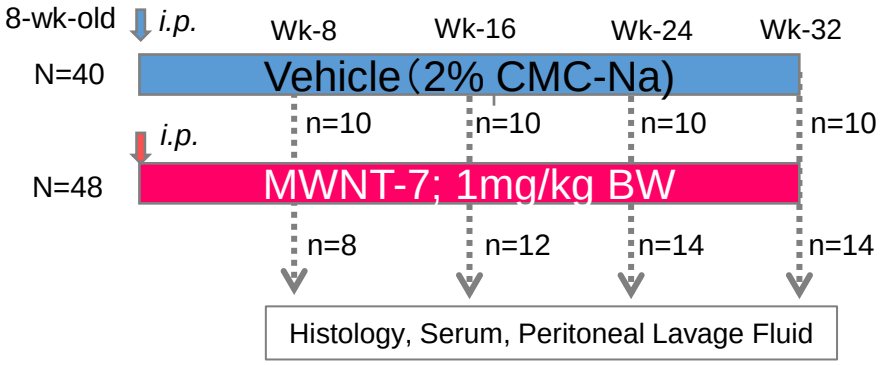

Carcinogenicity assessment test (up to 8 months)

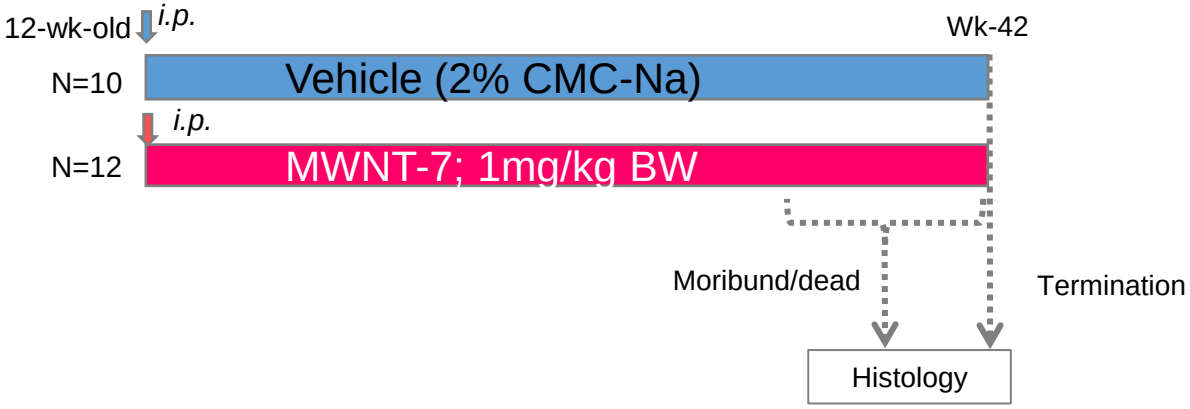

Figure S1 Characterization of MWNT-7 and the experimental design of Experiment 1

(A) Distribution of the length and diameter of MWCNTs was determined using SEM (FEI Quanta 250, Thermo Fischer Scientific Waltham, MA, USA) in our previous works[8].
(B) Representative SEM image of the MWCNT fibers.
(C) Experimental design of Experiment 1

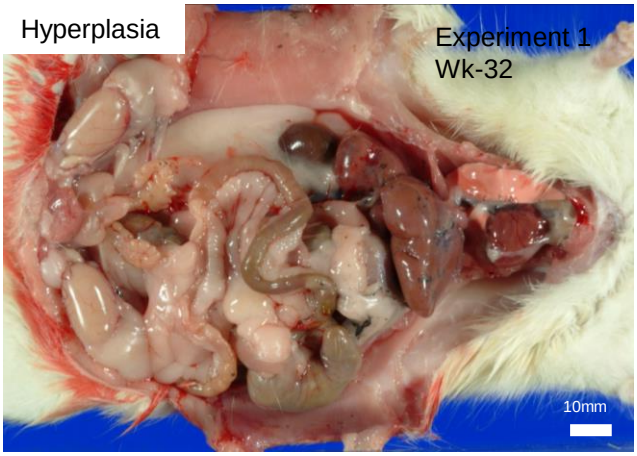

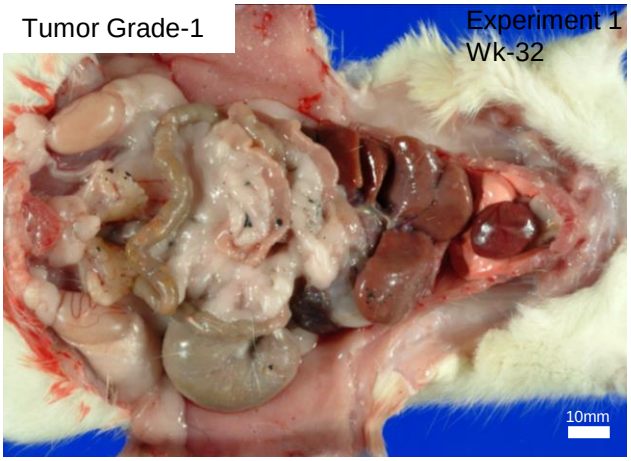

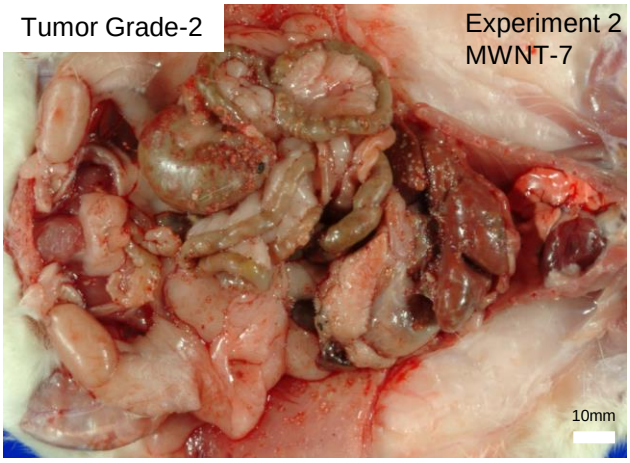

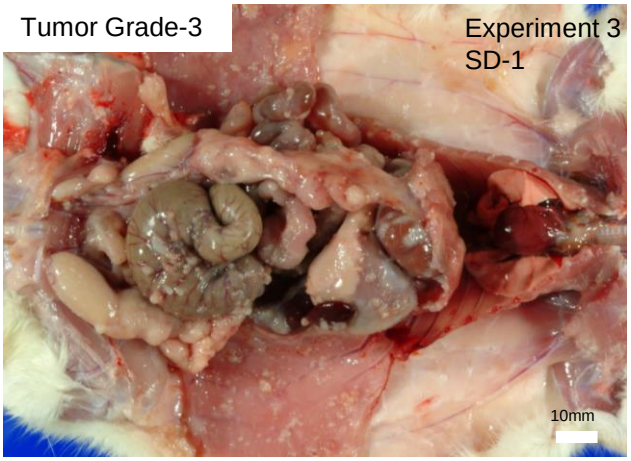

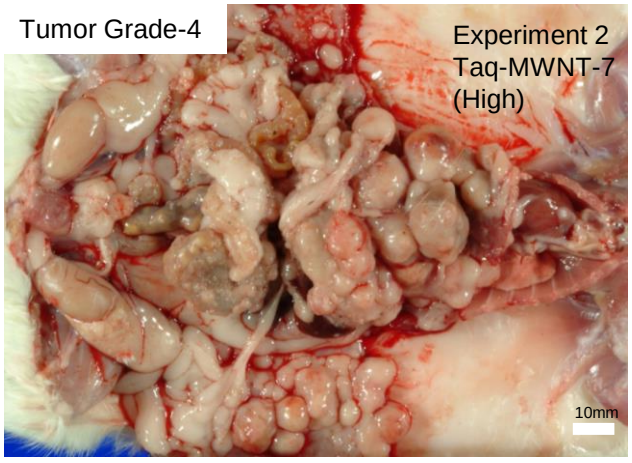

Figure S2 Grading criteria (gross findings)

Representative macroscopic appearance of the abdominal cavities of rat in each grade.

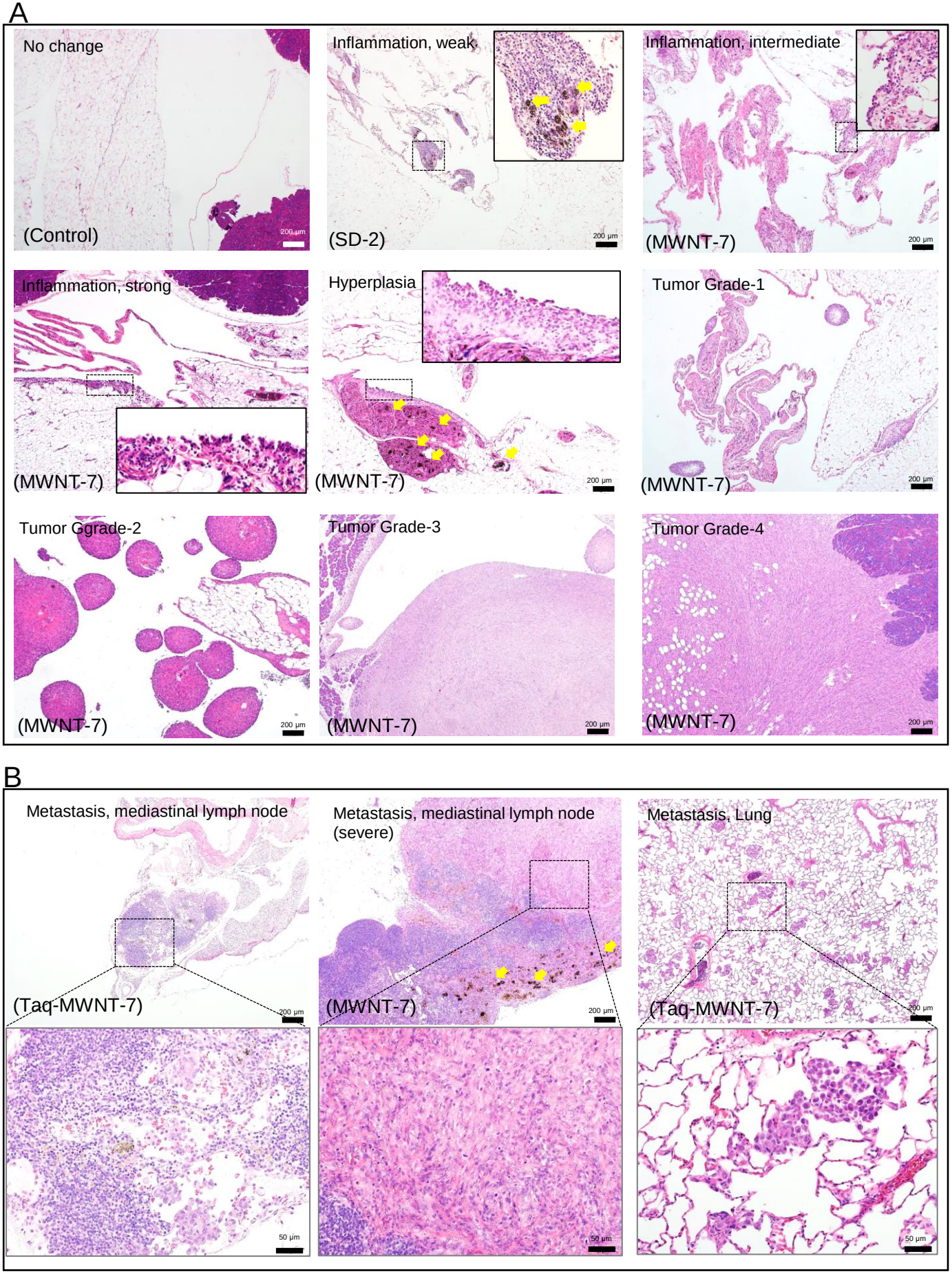

Figure S3 Grading criteria (histological findings)

(A) Representative image of each grade of the Total Consecutive Grade (Table 1; 0-8; No change; Inflammation-weak, -intermediate, -strong; Hyperplasia; Tumor Grade-1, -2, -3 and 4) in the mesothelium adjacent to the fat of the pancreas (H&E). Insets show high-powered views of the dotted rectangles. (B) Representative histology of the metastasis of mesothelioma in the mediastinal lymph node and the lung (H&E). Arrows show MWCNT fibers in macrophages and/or granulomas.

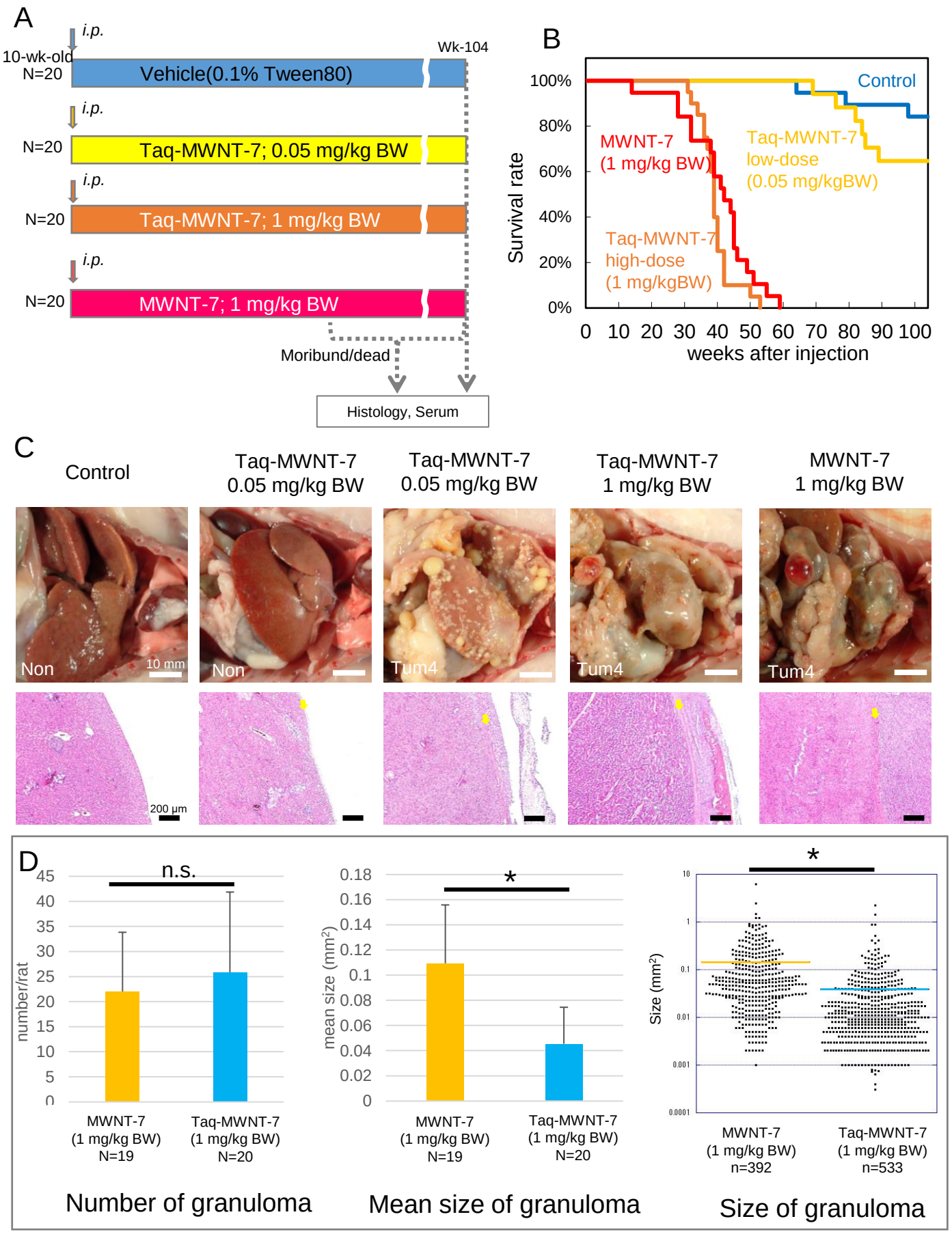

Figure S4 Overview of Experiment 2

(A) Experimental design of Experiment 2. (B) Kaplan-Meier survival curves in Experiment 2. Comparisons of the survival rate between the 2 groups were analyzed by Log-rank test. Significantly different between control and MWNT-7, control and Taq-MWNT-7 high-dose, Taq-MWNT-7 low-dose and MWNT-7, and Taq-MWNT-7 low-dose and Taq-MWNT-7 high-dose.

Figure S4 (Continued)

(C) Comparison of the fibrotic responses on the peritoneum in Experiment 2. Gross and microscopic images of the liver. Fibrosis of the outer serous layer of the liver was caused by MWCNT fibers. The shape of the liver was strikingly altered to be a grobe-like appearance, in 1 mg/kg BW of Taq-MWNT-7 or original MWNT-7 groups. The thickened fibrotic layer is shown by a yellow arrow. The degree of the thickness of the fibrosis was similar between these 2 groups. In 0.05 mg/kg BW of Taq-MWNT-7 group, no obvious thickening was found, regardless whether the mesothelioma developed.

(D) Comparison of the degree of the granulation occurring on the serosa between the original MWNT-7and Taq-MWNT-7 at the dose of 1 mg/kg BW. Number and size of the MWCNT-related granuloma on the serosa of the diaphragm, liver, stomach, pancreas and fat tissue flanking to the testis were measured using an image analyzer, Image J (NIH, Bethesda, MA, USA). The numbers of granuloma per rats were not different between the 2 groups (*left*; error bars show standard deviations), while the mean size of granuloma with standard deviations was significantly smaller in the Taq-MWNT-7 group than that in the original MWNT-7 (*middle*; error bars show standard deviations). There was a significant difference in the comparison of granuloma size obtained from all rats (*right*). n.s.: not significant

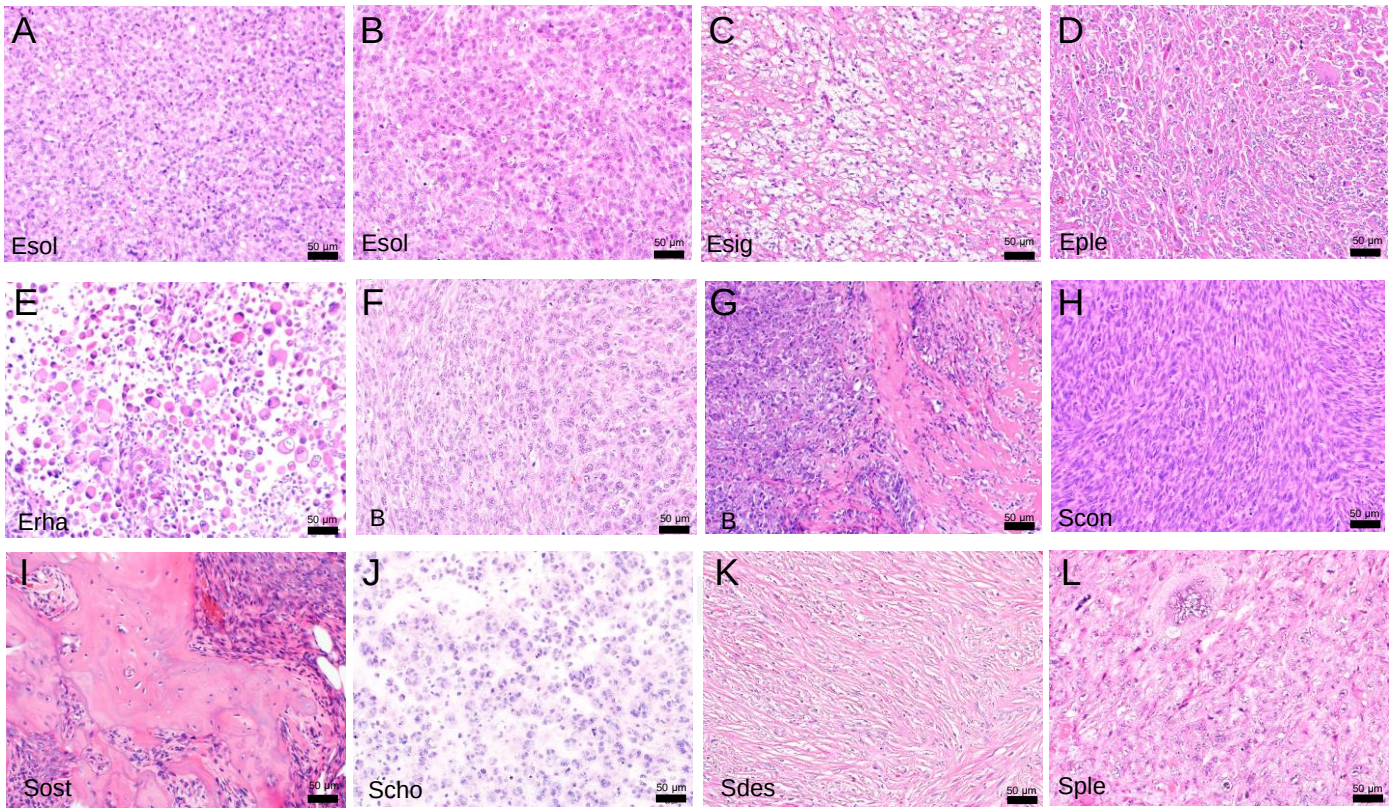

Figure S5. Representative histology of advanced mesotheliomas found in the 2 carcinogenicity tests. Epithelioid mesothelioma showing solid- (A and B), signet ring- (C), pleomorphic- (D) and rhabdoid- (E) structures. Biphasic mesothelioma (F and G). Sarcomatoid mesothelioma showiing conventional- (H), osteosarcomatous- (I), chondrosarcomatous (J), desmoplastic- (K) and pleomorphic- (L) structures.

A

Experiment 1

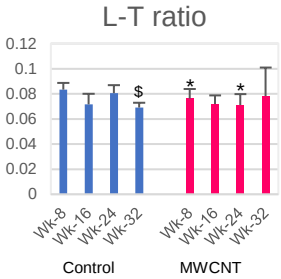

Experiment 2

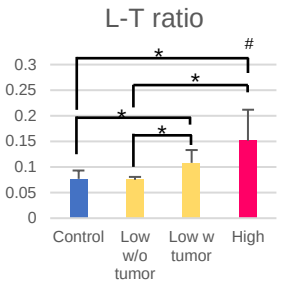

Experiment 3

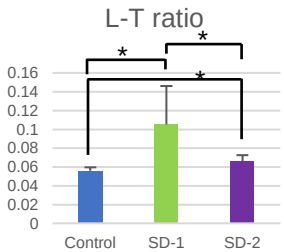

B

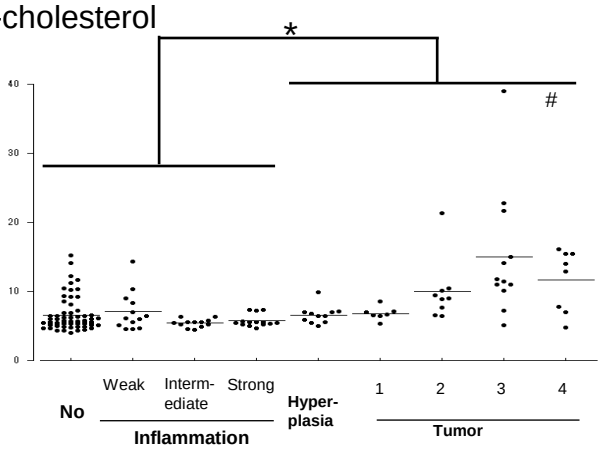

Rs=0.401 †

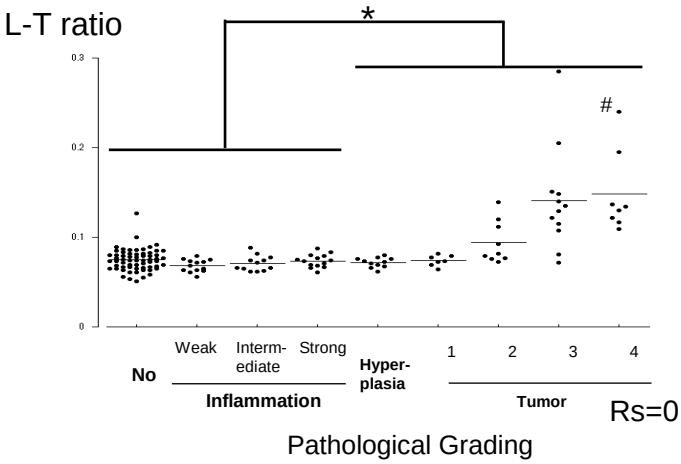

Rs=0.372 †

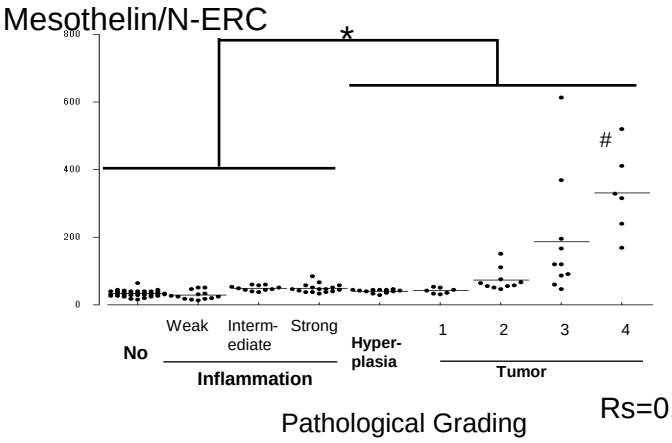

Rs=0.726 †

Figure S6 Serum levels of LDL-cholesterol, L-T ratio and mesothelin/N-ERC in the 3 experiments.

(A) Mean serum levels of L-T ratio with standard deviations in each experiment.
(B) Scattered plots for LDL-cholesterol, L-T ratio and mesothelin/N-ERC of integrated data of the 3 experiments in each pathological grade.
Rs: Spearman's Rho value.
* Significantly different between the 2 groups shown by a bracket.
$ Significant tendency of decrease with a time-dependency (Experiment 1)
# Significant tendency of increase according to a tumor burden (Experiment 2) or according to the histopathological grading (Integrated data).
† Significant correlation with the pathological grade (Total Consecutive Grade; Table 1; 0-8; No change; Inflammation-weak, -intermediate, -strong; Hyperplasia; Tumor Grade-1, -2, -3 and 4).

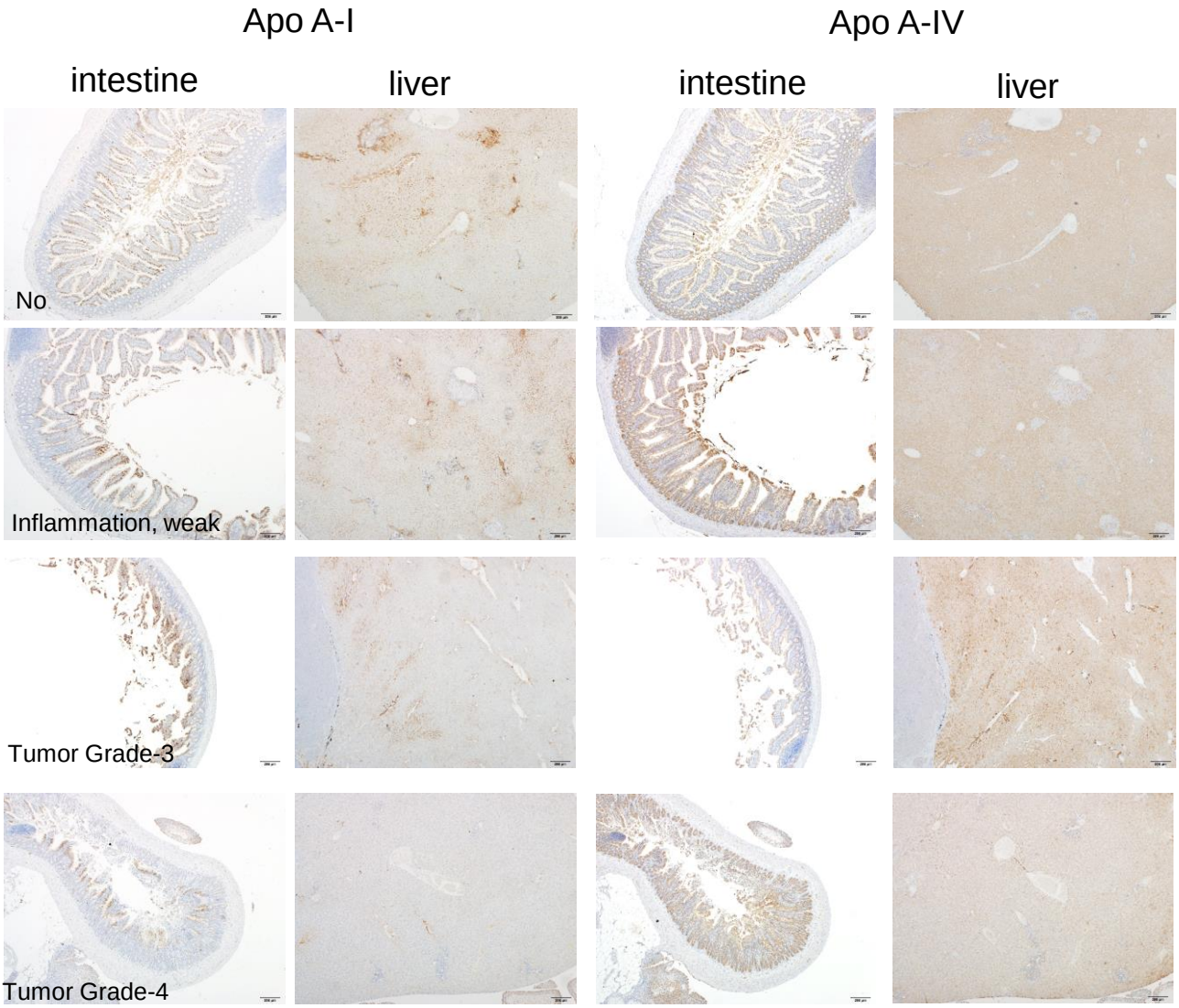

Figure S7 Immunostainings of apolipoproteins in the liver and intestine (jejunum) of rats each histological grade.

Representative images of the immunohistochemistry for Apo A-I and A-IV in each pathological grade. There was no apparent tendency concerning to intensities or locations of these signals between rats belonging to different pathological grades.

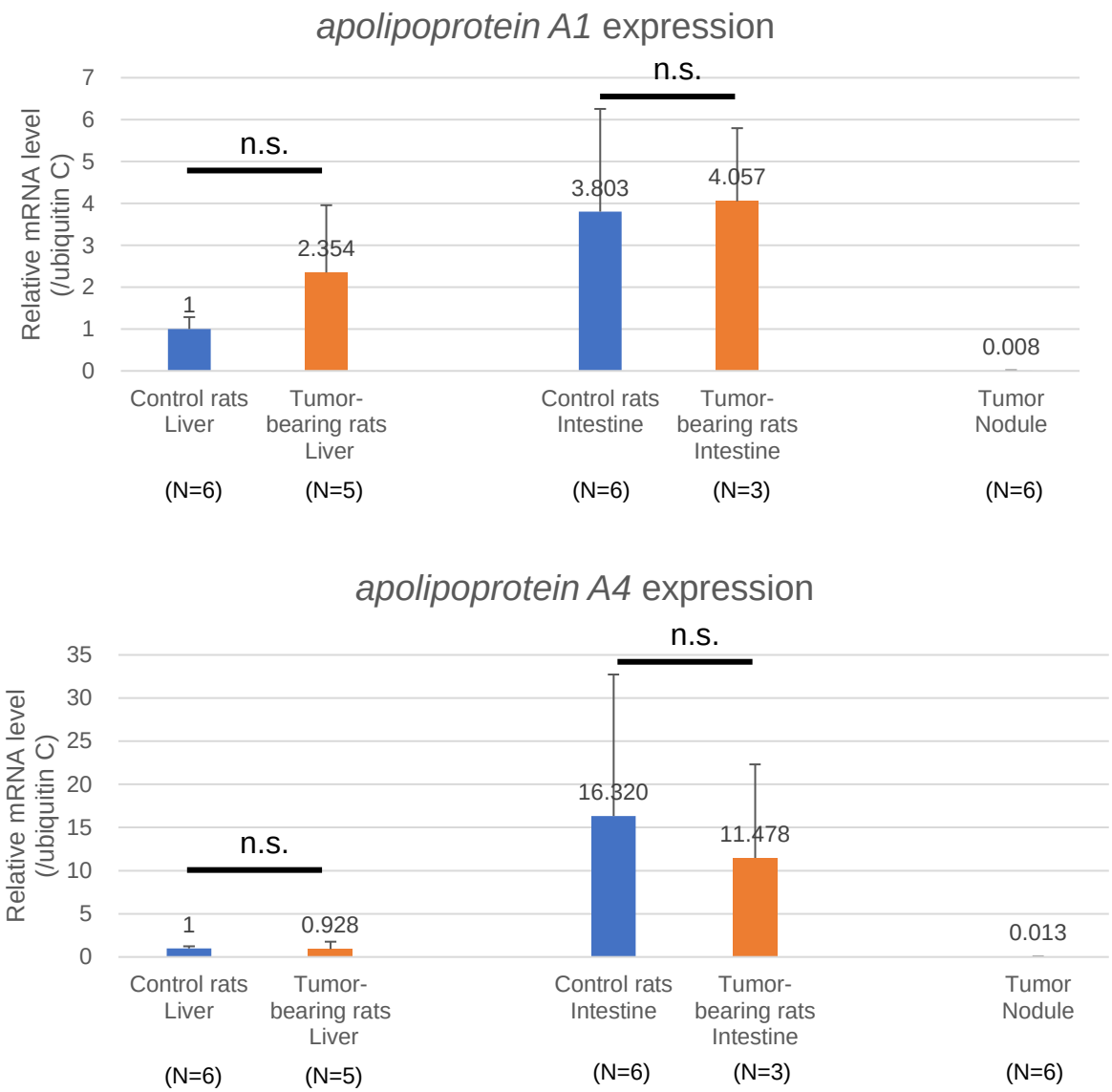

gene name	sequence of forward primer (5'-3')	sequence of reverse primer (5'-3')
apolipoprotein A1	GGCAGAGACTATGTGTCCCAGTTT	TTGAACCCAGAGTGTCCCAGTT
apolipoprotein A4	ACCCTCTTCCAGGACAAACTTG	CCTTGGTTAGATGTCCACTCAGTTG
ubiquitin c	ATCTAGAAAGAGCCCTTCTTGTGC	ACACCTCCCCATCAAACCC

Figure S8 Gene expressions of *apolipoproteins A1* and *A4* in the livers, intestines and tumor nodules in Experiment 2.

mRNA levels of *apolipoproteins A1* and *A4* (normalized to *ubiquitin c*) were shown by comparative values to the level in the liver of rats in the control groups.
At necropsies, samples were obtained from control or higher grade rats and snap frozen in liquid nitrogen. Quantitative RT-PCR was carried out by 7500 Real-Time PCR System (Thermo Fisher Scientific, Waltham, MA, USA).
DNA sequence of primers used here are summarized in a table.

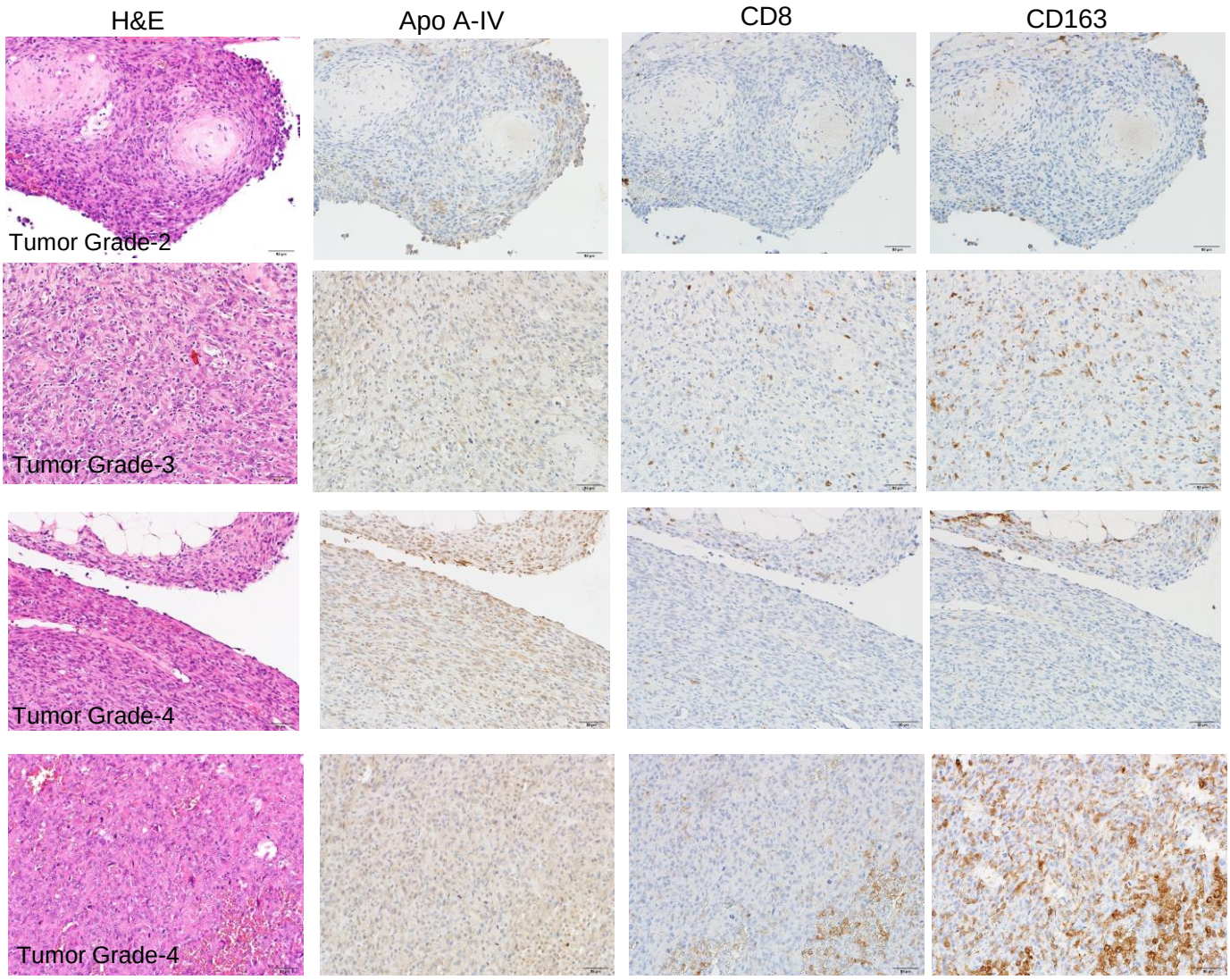

Figure S9 Immunohistochemical comparisons of localizations between Apo A-IV and immune cells

Representative immunohistochemistry for Apo A-IV, CD8 and CD163 in serial sections of the tumor nodules. The CD8- and CD163-positive cells were infiltrated in the tumor stroma of mesothelioma, especially in the higher grade animals (Tumor Grade-3 or -4). Each immune cells showed various infiltration patterns regardless of the deposition of Apo A-IV protein.